Published in final edited form as:
Clin Cancer Res. 2009 June 1; 15(11): 3770–3780. doi:10.1158/1078-0432.CCR-08-2306.

Therapeutic Targeting of ATP7B in Ovarian Carcinoma

Lingegowda S. Mangala[1], **Vesna Zuzel**[7], **Rosemarie Schmandt**[1], **Erik S. Leshane**[7], **Jyotsna B. Halder**[1], **Guillermo N. Armaiz-Pena**[1,4], **Whitney A. Spannuth**[1], **Takemi Tanaka**[6], **Mian M.K. Shahzad**[1,5], **Yvonne G. Lin**[1], **Alpa M. Nick**[1], **Christopher G. Danes**[1], **Jeong-Won Lee**[1,8], **Nicholas B. Jennings**[1], **Pablo E. Vivas-Mejia**[2], **Judith K. Wolf**[2], **Robert L. Coleman**[1], **Zahid H. Siddik**[2], **Gabriel Lopez-Berestein**[2], **Svetlana Lutsenko**[7], and **Anil K. Sood**[1,3]

[1]Department of Gynecologic Oncology, The University of Texas M. D. Anderson Cancer Center

[2]Department of Experimental Therapeutics, The University of Texas M. D. Anderson Cancer Center

[3]Department of Cancer Biology, The University of Texas M. D. Anderson Cancer Center

[4]Program in Cancer Biology, The University of Texas Graduate School of Biomedical Sciences at Houston

[5]Department of Obstetrics and Gynecology, Baylor College of Medicine

[6]Brown Institute of Molecular Medicine, The University of Texas Health Science Center, Houston, Texas

[7]Department of Biochemistry and Molecular Biology, Oregon Health and Science University, Portland, Oregon

[8]Department of Obstetrics and Gynecology, Samsung Medical Center, Sungkyunkwan University School of Medicine, Seoul, Korea

Abstract

Purpose—Resistance to platinum chemotherapy remains a significant problem in ovarian carcinoma. Here, we examined the biological mechanisms and therapeutic potential of targeting a critical platinum resistance gene, *ATP7B*, using both *in vitro* and *in vivo* models.

Experimental Design—Expression of ATP7A and ATP7B was examined in ovarian cancer cell lines by real-time reverse transcription-PCR and Western blot analysis. ATP7A and ATP7B gene silencing was achieved with targeted small interfering RNA (siRNA) and its effects on cell viability and DNA adduct formation were examined. For *in vivo* therapy experiments, siRNA was incorporated into the neutral nanoliposome 1,2-dioleoyl-*sn*-glycero-3-phosphatidylcholine (DOPC).

Results—*ATP7A* and *ATP7B* genes were expressed at higher levels in platinum-resistant cells compared with sensitive cells; however, only differences in ATP7B reached statistical significance. ATP7A gene silencing had no significant effect on the sensitivity of resistant cells to cisplatin, but ATP7B silencing resulted in 2.5-fold reduction of cisplatin IC_{50} levels and increased DNA adduct formation in cisplatin-resistant cells (A2780-CP20 and RMG2). Cisplatin was found to bind to the NH_2-terminal copper-binding domain of ATP7B, which might be a contributing factor to cisplatin

Requests for reprints: Anil K. Sood, Departments of Gynecologic Oncology and Cancer Biology, The University of Texas M. D. Anderson Cancer Center, 1155 Herman Pressler, Unit 1362, Houston, TX 77030. Phone: 713-745-5266; Fax: 713-792-7586; asood@mdanderson.org.

Disclosure of Potential Conflicts of Interest: No potential conflicts of interest were disclosed.

Note: Supplementary data for this article are available at Clinical Cancer Research Online (http://clincancerres.aacrjournals.org/).

The sponsors had no role in the study design, data collection and analysis, interpretation of the results, the preparation of the manuscript, or the decision to submit the manuscript for publication.

resistance. For *in vivo* therapy experiments, ATP7B siRNA was incorporated into DOPC and was highly effective in reducing tumor growth in combination with cisplatin (70-88% reduction in both models compared with controls). This reduction in tumor growth was accompanied by reduced proliferation, increased tumor cell apoptosis, and reduced angiogenesis.

Conclusion—These data provide a new understanding of cisplatin resistance in cancer cells and may have implications for therapeutic reversal of drug resistance.

Ovarian cancer has the highest mortality rate among all gynecologic malignancies (1). Following cytoreductive surgery, treatment with paclitaxel and platinum has become a recommended approach for initial chemotherapy (2). Current combination chemotherapy regimens produce complete remission in up to 80% of patients with advanced ovarian cancer. However, despite these initial high response rates, most patients suffer relapse and require treatment with multiple subsequent chemotherapy regimens (3). Successful management of advanced or recurrent gynecologic malignancies is often difficult due to both intrinsic and acquired resistance of cancer cells to chemotherapeutic agents (4–6). Therefore, novel strategies for overcoming resistance are needed.

Translational Relevance

Resistance to platinum chemotherapy remains a significant problem in ovarian carcinoma. Although several potential targets have been identified, an understanding of the underlying mechanisms and practical approaches for reversing resistance has been largely lacking. Here, we used a highly efficient method of systemic small interfering RNA delivery using neutral nanoliposomes to target a key gene involved in cisplatin resistance and provide novel insights into its mechanism of action. These findings offer new opportunities for development of molecular therapies to reverse chemotherapy resistance.

Cisplatin exerts its cytotoxicity by forming platinum-DNA adducts that arrest the cell in G_1, S, or G_2-M phases of the cell cycle, which ultimately lead to programmed cell death. Enhanced DNA repair, increased intracellular levels of glutathione or metallothionein, and drug accumulation may lead to resistance of cells to cisplatin (7–11). In addition, decreased influx or increased efflux of cisplatin may contribute to resistance. However, the mechanisms underlying these drug accumulation defects are poorly understood. Recent studies suggest that the transporter that mediates copper uptake and efflux may also regulate the cellular pharmacology of cisplatin (12,13). Specifically, two copper transporters, ATP7A and ATP7B, are expressed at higher levels in platinum-resistant cell lines (14–17) and have been functionally implicated in resistance to several platinum agents, including cisplatin, carboplatin, and oxaliplatin (17). ATP7B was also shown to be overexpressed in several solid tumors, including gastric, breast, esophageal, hepatocellular, colorectal, uterine, and oral squamous cell carcinomas (18–24). ATP7A and ATP7B are members of the P-type ATPase family of transporters and are the product of genes affected in two disorders of copper homeostasis in humans, Menkes disease and Wilson's disease, respectively (25,26). The primary function of ATP7A and ATP7B is to transport copper into the lumen of the *trans*-Golgi network (TGN) for the biosynthesis of copper-dependent enzymes and to facilitate export of excess copper from the cell by sequestering copper into exocytic vesicles (27). Cu-ATPases bind copper at their large NH_2-terminal domain and then transfer copper across the membrane using the energy of ATP hydrolysis; elevated copper stimulates the Cu-ATPase activity and causes intracellular trafficking of these transporters from the TGN to exocytic vesicles.

To date, the ability to target chemotherapy resistance genes has been limited. We have recently developed highly efficient methods for *in vivo* gene silencing using small interfering RNA (siRNA) incorporated into neutral nanoliposomes, 1,2-dioleoyl-*sn*-glycero-3-

phosphatidylcholine (DOPC; refs. 28, 29). Here, we used this technology to silence key cisplatin resistance genes and show antitumor efficacy with ATP7B gene silencing.

Materials and Methods

Cell lines and culture

The derivation, source, and propagation of human epithelial ovarian cancer cell lines, such as cisplatin-sensitive (A2780-PAR) and platinum-resistant (A2780-CP20 and RMG2) epithelial ovarian cancer cell lines, were maintained as previously described (30). The A2780-CP20 cell line was developed by sequential exposure of the A2780 cell line to increasing concentrations of cisplatin. All experiments were done with 70% to 80% confluent cultures.

ATP7A and ATP7B gene silencing by siRNA

siRNA constructs targeted to ATP7A and ATP7B were designed and purchased from Qiagen. The target sequences were 5′-CTGGACCGGATTGTTAATTAT-3′ (for ATP7A) and 5′-CCAATTGATATTGAGCGGTTA-3′ (for ATP7B). *In vitro* transient transfection was done as described previously (28). Briefly, cells were transfected with ATP7A- and/or ATP7B-specific or scrambled (control) siRNA using RNAiFect reagent (Qiagen). At selected time intervals, cells were harvested to measure mRNA and protein levels of ATP7B using reverse transcription-PCR and Western blot analysis, respectively. An oligonucleotide sequence that did not have homology to any human mRNA (scrambled siRNA as determined by a National Center for Biotechnology Information BLAST search) served as a control.

Reverse transcription-PCR

Total RNA was isolated by using Qiagen RNeasy kit. cDNA was synthesized by using the SuperScript First-Strand kit (Invitrogen) as per the manufacturer's instructions. cDNA was subjected to PCR using specific primers 5′-CTGGCAAGGCAGAAGTAAGG-3′ (sense) and 5′-TGCAAAGTGGTGGTCCATAA-3′ (antisense) for ATP7A and 5′-GGTGTTCTCTCCGTGTTGGT-3′ (sense) and 5′-GGCTGCACAGGAAAGACTTC-3′ (antisense) for ATP7B; *β-actin* was used as a housekeeping gene. PCR was done with 5 to 25 μg of reverse-transcribed RNA and 100 ng/μL of sense and antisense primers in a total volume of 20 μL. Each cycle consisted of 45 s of denaturation at 94°C, 1 min of annealing at 55°C, and 45 s of elongation at 72°C (22 cycles). Amplified PCR products were analyzed by electrophoresis on 1% agarose gel with Tris-borate-EDTA buffer and visualized under UV light after staining with ethidium bromide.

Western blot analysis

Cells grown to 80% confluence were harvested and lysed in modified radioimmunoprecipitation assay buffer (50 mmol/L Tris, 150 mmol/L NaCl, 1% Triton X-100, 0.5% deoxycholate, 25 μg/mL leupeptin, 10 μg/mL aprotinin, 2 mmol/L EDTA, 1 mmol/L sodium orthovanadate) as previously described (29). To prepare lysate from snap-frozen tissue of *in vivo* tumors, ~30 mm^3 slices of tissue were homogenized in modified radioimmunoprecipitation assay buffer and the lysates were centrifuged at 12,500 rpm for 20 min at 4°C. Total protein concentration of the supernatant was determined using the bicinchoninic acid protein assay reagent kit (Pierce). Protein (30-50 μg) was separated by SDS-PAGE on a 6% gel and electrophoretically transferred onto a nitrocellulose membrane. The blots were blocked for 1 h in 5% milk powder in TBST [10 mmol/L Tris (pH 8), 150 mmol/L NaCl, 0.05% Tween 20] and incubated at 4°C overnight with anti-ATP7A and anti-ATP7B antibodies (Novus Biologicals) at dilutions of 1:1,000 and 1:500, respectively. ATP7B antibody recognized a band at 165 kDa, representing ATP7B protein, and also recognized an unknown band at ~195 kDa. After being washed in TBST, blots were probed with horseradish

peroxidase–conjugated goat anti-rabbit antibodies (GE Healthcare) in TBST for 1 h at room temperature. Immunoreactive proteins were visualized using enhanced chemiluminescence (Perkin-Elmer). All membranes were stripped and reprobed with an anti–β-actin antibody (Sigma-Aldrich) at a dilution of 1:2,000 to ensure even loading of proteins.

Cytotoxicity [3-(4,5-dimethylthiazol-2-yl)-2,5-diphenyltetrazolium bromide] assay

The cytotoxicity of both sensitive and resistant cells to cisplatin was determined by measuring their ability to reduce the tetrazolium salt [3-(4,5-dimethylthiazol-2-yl)-5-(3-carboxymethoxyphenyl)-2-(4-sulfophenyl)-2*H*-tetrazolium, inner salt] to a formazan, as described previously (31). Briefly, A2780-PAR and A2780-CP20 cells were plated at 2×10^3 per well in 96-well plate and allowed to adhere overnight. Cells were transfected with control or ATP7A- and/or ATP7B-targeted siRNAs. After 48 h of transfection, the cells were exposed to increasing concentrations of CDDP (*cis*-diamminedichloroplatinum or cisplatin; final concentration range, 0.01-32 μmol/L; LKT Laboratories). After 72 h of cisplatin exposure, cells were incubated with 0.15% 3-(4,5-dimethylthiazol-2-yl)-2,5-diphenyltetrazolium bromide (MTT) for 2 h at 37°C. The supernatant was removed and cells were dissolved in 100 μL DMSO. The absorbance at 570 nm was recorded, and the IC_{50} was determined.

Immunocytochemistry of ATP7B

Tumor cells (80-90% confluent) were grown on coverslips (1:20 dilution) for 24 to 48 h at 37°C and treated with 50 μmol/L bathocuproinedisulfonic acid disodium salt (BCS) to decrease copper levels and then treated with $CuCl_2$ or CDDP (2 or 10 μmol/L) at 37°C for 1 h. Cells were fixed by immersing in acetone for 30 s at −20°C and then blocked overnight at 4°C in a blocking buffer containing 1% gelatin/1% bovine serum albumin in PBS. Cells were incubated with a primary antibody raised against the NH_2-terminal domain of ATP7B and syntaxin-6 (TGN marker) at room temperature for 1 h (each antibody at a 1:500 dilution). After being washed thrice with PBS for 30 min, cells were incubated for 1 h with fluorescently labeled secondary antibodies (Alexa Fluor 488 donkey anti-rat for ATP7B and Alexa Fluor 555 donkey anti-mouse for syntaxin-6; Molecular Probes, Invitrogen). Cells were washed again with PBS as described above and then mounted using mounting medium containing 4′,6-diamidino-2-phenylindole (Vector Laboratories). Images were analyzed using 100× with a Zeiss confocal scanning microscope (Carl Zeiss); colocalization of ATP7B and syntaxin was evaluated using multiple images and Zeiss software package (track option).

DNA adduct formation assay

Eighty percent of confluent cells were incubated with cisplatin at concentrations up to 20 μmol/L at 37°C for 4 h. Cells were centrifuged at 1,000 rpm for 5 min and washed twice with ice-cold PBS. Cell pellets were digested overnight at 55°C with 1 mol/L benzethonium hydroxide (0.075 mL). Samples were then acidified with 0.1 mL of 1 N HCl and the platinum content was determined in a flame atomic absorption spectrometer (SpectrAA300, Varian). To determine protein content, cell pellets from parallel incubations were first lysed with lysis buffer and then the protein content was determined by bicinchoninic acid method. The experiment was repeated for a total of three times, and the mean value was recorded.

Binding of cisplatin to the NH_2-terminal domain of ATP7B (N-ATP7B)

N-ATP7B (previously referred as N-WNDP) was expressed and purified as a fusion protein with maltose binding protein as previously described (32). Before binding experiments, purified protein was fully reduced with 100 μmol/L DTT and then dialyzed overnight using the buffer containing 25 mmol/L phosphate and 150 mmol/L NaCl (pH 7.5). Copper or cisplatin was added to the N-ATP7B in increasing molar ratios up to 60-fold excess over protein (10-fold excess over metal-binding sites) for 10 min at room temperature. Next, 7-diethylamino-3-

(4′-maleimidylphenyl)-4-methylcoumarin (CPM; Invitrogen) was added in the dark for 5 min (in equimolar concentrations to metal-binding cysteines) and quenched with 20 μmol/L glutathione. Samples were run on a 12% Laemmli gel, and fluorescent images were taken using a FluorChem 5500 (Alpha-Innotech Corp.). Gels were then fixed, stained with Coomassie, and imaged again. The intensity of CPM labeling was normalized to protein levels by densitometry and expressed as a percentage of protein labeling in the absence of cisplatin. This experiment was replicated thrice, and the mean value was recorded.

Overexpression of N-ATP7B in A2780-PAR cells

After 24 h of plating, cells were transfected with empty vector pTriEx-cDNA or pTriEx-N-ATP7B cDNA (ATP7B-WND) using Lipofectamine 2000 (Invitrogen) according to the manufacturer's protocol. Briefly, cDNA and Lipofectamine solution (1:2.5 ratio) were diluted with serum-free medium and two solutions were mixed and incubated for 20 min at room temperature. This mixture was added to cells and serum-free medium was replaced with regular serum-containing medium after 6 to 8 h of incubation. After 48 h, cells were trypsinized and plated in 96-well plates. After attachment of cells, cisplatin was added to the cells and incubated for 72 h at 37°C. Cytotoxicity was determined by MTT assay as described above. The extent of protein overexpression was also confirmed by Western blot analysis.

Liposomal siRNA preparation

For *in vivo* delivery, siRNA was incorporated into DOPC as previously described (28). Briefly, siRNA and DOPC were mixed at a ratio of 1:10 (w/w) siRNA/DOPC in excess tertiary butanol. Tween 20 was added to the mixture at the ratio of 1:19 (Tween 20:siRNA/DOPC). After vortexing, the mixture was frozen in an acetone/dry ice bath and lyophilized. Before *in vivo* administration, this mixture was hydrated with 0.9% saline to a concentration of 25 μg/mL and 200 μL of mixture were used per injection.

Orthotopic model of ovarian cancer and tissue processing

Female athymic nude mice (NCr-nu) were purchased from the National Cancer Institute-Frederick Cancer Research and Development Center (Frederick, MD). All mice were housed and maintained under specific pathogen-free conditions in facilities approved by the American Association for Accreditation of Laboratory Animal Care and in accordance with current regulations and standards of the U.S. Department of Agriculture, U.S. Department of Health and Human Services, and NIH. All studies were approved and supervised by the University of Texas M. D. Anderson Cancer Center Institutional Animal Care and Use Committee. All mice were used in these experiments when they were 8 to 12 wk old.

Before injection, tumor cells were washed twice with PBS, detached by 0.1% cold EDTA, centrifuged for 7 min, and reconstituted in HBSS (Invitrogen). Cell viability was confirmed by trypan blue exclusion. Tumors were established by i.p. injection of either 1.0×10^6 A2780-CP20 or 3.0×10^6 RMG2 cells. Once established, this tumor model reflects the growth pattern of advanced ovarian cancer (33,34).

Long-term therapy experiments were done using two platinum-resistant ovarian cancer cell lines: A2780-CP20 and RMG2. To assess the effects of siRNA therapy on tumor growth, treatment was initiated 1 wk after i.p. injection of tumor cells. Mice were divided into five groups ($n = 10$ mice per group): (*a*) empty liposome (DOPC; vehicle), (*b*) control siRNA-DOPC (150 μg/kg i.p. twice weekly), (*c*) control siRNA-DOPC + cisplatin (160 μg/mouse i.p. weekly), (*d*) ATP7B siRNA-DOPC (150 μg/kg i.p. twice weekly), and (*e*) ATP7B siRNA-DOPC + cisplatin (doses same as individual treatments). Treatment was continued until control mice became moribund (typically 4-6 wk following tumor cell injection). At the time of sacrifice, mouse weight, tumor weight, number of nodules, and distribution of tumors were

recorded. Tissue samples were snap frozen for lysate preparation or fixed in formalin for paraffin embedding. The individuals who did the necropsies, tumor collections, and tissue processing were blinded to the treatment group assignments.

Immunohistochemistry

Proliferating cell nuclear antigen (PCNA), terminal deoxynucleotidyl transferase–mediated dUTP nick end labeling (TUNEL) staining, and microvessel density (MVD) were done using formalin-fixed, paraffin-embedded tumor sections (8 μm thickness) as previously described (35). Briefly, after deparaffinization and rehydration, antigen retrieval was done using citrate buffer (0.1 mol/L; pH 6.0) in a microwave. Endogenous peroxidase and nonspecific epitopes were blocked with 3% H_2O_2/methanol for 12 min and 5% normal horse serum and 1% normal goat serum for 20 min. Sections were incubated with primary anti-PCNA (PC-10, mouse IgG; Dako Corp.) or anti-CD31 (Pharmingen) overnight at 4°C and secondary horseradish peroxidase–conjugated antibody (Serotec Bioproducts) for 1 h at room temperature. Horseradish peroxidase was detected with 3,3′-diaminobenzidine (Phoenix Biotechnologies) substrate for 5 min, washed, and counterstained with Gill's no.3 hematoxylin (Sigma-Aldrich) for 15 s and mounted.

To quantify apoptosis, we did TUNEL staining on 8-μm-thick paraffin-embedded tumor slides as previously described (35). Briefly, after deparaffinization, slides were treated with proteinase K (1:500) and a positive control slide was treated with DNase. Endogenous peroxidase activity was blocked with 3% H_2O_2 in methanol. After being rinsed with TdT buffer (30 mmol/L Trizma, 140 mmol/L sodium cacodylate, 1 mmol/L cobalt chloride), slides were incubated with terminal transferase (1:400; Roche Diagnostics) and biotin-16-dUTP (1:200; Roche Diagnostics) and blocked with 2% bovine serum albumin. Slides were then incubated with peroxidase streptavidin (1:400) at 37°C for 40 min, visualized with 3,3′-diaminobenzidine chromogen, and counterstained with Gill's hematoxylin. The apoptotic and proliferative indices and MVD were determined by the number of positive cells in five randomly selected high-power fields exclusive of necrotic areas. To quantify PCNA expression, MVD, and apoptotic cells, the number of positive cells (3,3′-diaminobenzidine staining) was counted in 10 random 0.159 mm^2 fields at ×100 magnification. All staining was quantified by two investigators in a blinded fashion (35).

ELISA

To examine the levels of vascular endothelial growth factor (VEGF) in ATP7B-silenced tumors, we did ELISA using the VEGF Quantikine kit from R&D Diagnostics according to the manufacturer's instructions. The experiment was done twice.

Statistics

For animal experiments, 10 mice were assigned per treatment group. To judge the necessary sample size for proposed experiments, we considered a two-way ANOVA model. For an effect size (ratio of fixed effect and residual SD) of 1.3, this sample size will be sufficient to provide 80% power for a test at significance level of 0.05. Mouse and tumor weights and the number of tumor nodules for each group were compared using Student's *t* test (for comparisons of two groups). Statistical analyses were done using Statistical Package for the Social Sciences 12.0 for Windows (SPSS, Inc.). A two-tailed $P \leq 0.05$ was deemed statistically significant.

Results

In vitro effects of ATP7A and ATP7B silencing

Before initiating *in vivo* experiments, we first identified the cisplatin IC_{50} levels for multiple ovarian cancer cell lines (Supplementary Table S1). The A2780-CP20, IGROV-CP20, and RMG2 cell lines are resistant to cisplatin with IC_{50} levels of ≥12 μmol/L. Next, we examined expression of ATP7A and ATP7B in the ovarian cancer cell lines using quantitative real-time reverse transcription-PCR. Although levels of both genes were higher in the cisplatin-resistant cells, only ATP7B reached statistical significance (Supplementary Fig. S1A). Both ATP7A and ATP7B were previously implicated in resistance to cisplatin (16, 17). Consequently, to determine which of these transporters contributes to drug resistance, we used siRNA targeted against ATP7A or ATP7B. Transfection of A2780-CP20 cells with the targeted siRNAs resulted in decreased protein levels by 73% (ATP7A) and 68% (ATP7B) at 48 hours (Fig. 1A). Similarly, mRNA expression was decreased for both genes at 48 hours (Supplementary Fig. S1B and C). Next, the effects of ATP7A or ATP7B silencing were assessed on tumor cell sensitivity to cisplatin using the MTT assay. ATP7A gene silencing had no significant effect on sensitivity to cisplatin in either cell line (Fig. 1B). In contrast, ATP7B gene silencing increased sensitivity to cisplatin by 5.5-fold ($P < 0.01$) in the A2780-PAR cells (Fig. 1B) and 2.5-fold ($P < 0.05$) in the A2780-CP20 cells (Fig. 1B). The combination of ATP7A and ATP7B gene silencing showed effects similar to ATP7B siRNA alone, suggesting that ATP7A down-regulation did not contribute significantly to sensitization of the resistant A2780-CP20 cells to cisplatin. Therefore, for all subsequent studies, we focused on the contribution of ATP7B to platinum resistance using *in vivo* orthotopic mouse models of ovarian cancer. ATP7A and ATP7B siRNA sequences did not show cross-reactivity against each other (data not shown). Trypan blue dye assay confirmed that transfection of cells with siRNAs did not affect cell viability after 48 hours of transfection (Supplementary Fig. S1D), suggesting that siRNA was not toxic to cells.

Cisplatin does not alter intracellular localization of ATP7B

To better understand the mechanisms by which copper-transporting ATPases mediate cisplatin resistance, we examined the effect of cisplatin on ATP7B in A2780-CP20 cells in more detail. In hepatic cells, the efflux of copper by ATP7B is associated with the trafficking of ATP7B from the TGN to vesicles (36). Consequently, we asked whether cisplatin induces ATP7B trafficking from the TGN, a step that precedes metal efflux. To better visualize the potential effect of cisplatin and avoid metal competition, cells were first depleted of copper with the copper chelator BCS and then treated with cisplatin (Fig. 2). As expected, in copper-depleted cells, ATP7B was found in the perinuclear compartment where it colocalized with the TGN marker syntaxin-6. Treatment with cisplatin or copper (either 2 or 10 μmol/L) did not produce a noticeable change in the ATP7B pattern (Fig. 2A). ATP7B remained colocalized with syntaxin-6 and remained in a perinuclear location, suggesting that ATP7B largely colocalized with the TGN marker under all experimental conditions.

To verify the lack of ATP7B trafficking in response to cisplatin in A2780-CP20 cells, we evaluated colocalization between ATP7B and syntaxin using multiple images and Zeiss software package. Trafficking in response to copper in HepG2 was used as a positive control (Fig. 2B). Following treatment with BCS, ATP7B showed colocalization with the TGN marker in both cell types. This colocalization was lost in the HepG2 cells in response to copper elevation, indicative of trafficking. However, there was no significant change in the colocalization of ATP7B and the TGN marker in the A2780-CP20 cells (Fig. 2B).

ATP7B silencing increases DNA adduct formation

Although ATP7B does not show noticeable trafficking, it may increase cell resistance to cisplatin either through a slow sequestration of drug in the TGN or by binding cisplatin at its metal-binding sites and rendering the drug unavailable. In either case, down-regulation of ATP7B would be expected to increase the intracellular concentration of "active" cisplatin. To determine the effects of ATP7B gene silencing, we compared platinum content and DNA adduct formation in A2780-PAR and A2780-CP20 cells (Fig. 3A). ATP7B gene silencing had no effect on whole-cell platinum accumulation (data not shown) consistent with the lack of ATP7B trafficking and metal efflux. However, ATP7B silencing resulted in a 30% increase in DNA adduct formation in both A2780-PAR and A2780-CP20 cells ($P < 0.05$ versus untreated and control siRNA–treated cells; Fig. 3A), suggesting a role for ATP7B in regulating intracellular distribution of cisplatin.

Cisplatin binds to the NH_2-terminal domain of ATP7B

ATP7B has a large NH_2-terminal domain (N-ATP7B) that contains six copper-binding sites (37). In addition, N-ATP7B can bind other metals, such as zinc, although with lower affinity (38). Therefore, we next examined the ability of N-ATP7B to bind cisplatin. Previously, binding of copper to recombinant N-ATP7B was shown to protect metal-coordinating cysteine residues from labeling with the fluorescent CPM (39). Consequently, we tested whether such protection occurs in the presence of increasing concentrations of cisplatin (Fig. 3B). Incubation of N-ATP7B with both copper and cisplatin decreased fluorescent labeling, suggesting that both metals can interact with the metal-binding sites in ATP7B. Such binding to overexpressed ATP7B may contribute to increased resistance of A2780-CP20 cells to cisplatin. To examine whether binding of cisplatin to the NH_2-terminal domain of ATP7B is sufficient to increase resistance to cisplatin, we overexpressed the recombinant N-ATP7B in cisplatin-sensitive A2780-PAR cells and this resulted in a 2-fold increase in resistance ($IC5_0$) of the A2780-PAR cells to cisplatin ($P < 0.03$; Fig. 3C). When A2780-PAR cells were transfected with an empty vector (pTriEx), as expected, no ATP7B protein was expressed (A2780-PAR-pTriEx) compared with A2780-CP20 cells. Overexpression of recombinant N-ATP7B (70 kDa) in the A2780-PAR cells (A2780-PAR-WND) produced protein levels that were comparable with those of the full-length ATP7B in A2780-CP20 cells (Fig. 3D) and yielded increased resistance, suggesting that binding of the NH_2-terminal domain is one of the contributing factors to resistance. We have attempted to isolate the His-tagged N-ATP7B from cells treated with fluorescent cisplatin to evaluate stoichiometry of cisplatin binding; however, the sensitivity of our assays was insufficient for such measurements.

In vivo effects of ATP7B inhibition on ovarian carcinoma

The therapeutic potential of ATP7B gene silencing for reversing platinum resistance was tested *in vivo* using ATP7B siRNA delivery by DOPC (28). Before therapy experiments, we established the duration of ATP7B gene silencing following i.p. administration of ATP7B siRNA in DOPC. Nude mice bearing A2780-CP20 tumors were injected with a single dose of ATP7B siRNA-DOPC (150 μg/kg), and tumors were harvested after 24, 48, 72, and 96 hours (Fig. 4A). ATP7B siRNA-DOPC reduced the expression of ATP7B (60%) by 48 hours and returned to baseline levels at 96 hours. Based on these results, we administered ATP7B siRNA-DOPC twice weekly for subsequent therapy experiments. To check for nonspecific inflammatory responses produced by siRNA *in vivo*, we measured cytokine levels in plasma 2 hours after the i.v. administration of normal saline, empty liposome (DOPC), control siRNA-DOPC, or ATP7B siRNA-DOPC into mice. There was no significant induction of IFN-γ, interleukin (IL)-1β, IL-2, IL-4, IL-5, IL-10, and tumor necrosis factor-α in any of the groups (Supplementary Table S2), suggesting that administration of siRNA did not induce nonspecific inflammatory responses, which agreed with previous reports (40).

To simulate treatment of advanced small-volume disease, we initiated therapy 1 week after tumor cell injection using the A2780-CP20 and RMG2 models (Fig. 4B). Mice were divided into the following five groups ($n = 10$ mice per group): (*a*) empty liposomes, (*b*) control siRNA-DOPC, (*c*) control siRNA-DOPC + cisplatin, (*d*) ATP7B siRNA-DOPC, and (*e*) ATP7B siRNA-DOPC + cisplatin. All of the animals were sacrificed when animals in any group appeared moribund (3-5 weeks of therapy depending on the cell line). Treatment with ATP7B siRNA-DOPC alone resulted in 40% to 60% reduction in tumor weight in both models compared with treatment with either empty liposome or control siRNA-DOPC ($P < 0.05$; RMG2 tumors). Combination therapy (ATP7B siRNA-DOPC and cisplatin) resulted in even greater reduction (70% and 88% in the A2780-CP20 and RMG2 models, respectively; Fig. 4B) in tumor weight than either cisplatin/control siRNA-DOPC or ATP7B siRNA-DOPC alone ($P < 0.05$ versus either empty liposome or control siRNA-DOPC for A2780-CP20 and $P < 0.001$ versus either control siRNA-cisplatin or ATP7B siRNA-DOPC in RMG2 tumors).

To further evaluate the effects of ATP7B therapy on tumor growth inhibition, we analyzed tumor incidence, tumor weight distribution, and number of nodules. Again, combination therapy showed the greatest effect with 60% fewer tumor nodules ($P < 0.05$ versus empty liposome and control siRNA-DOPC groups) in A2780-CP20 and 75% fewer ($P < 0.05$ versus empty liposome and control siRNA-DOPC groups) in RMG2 cells (Table 1; Supplementary Fig. S2). There was no obvious toxicity noted in the animals during therapy experiments, as assessed by changes in behavior, feeding habits, and mobility. The mean body weight was also similar between the treatment groups (data not shown).

Effect of ATP7B silencing on tumor proliferation, apoptosis, and angiogenesis

To explore possible mechanisms underlying the observed inhibition of tumor growth, we examined the effects of ATP7B silencing on tumor cell proliferation and apoptosis by using PCNA and TUNEL staining. In the A2780-CP20 tumor model, treatment with ATP7B siRNA-DOPC alone reduced proliferation by 57% ($P < 0.05$), and combination therapy further reduced it by 75% ($P < 0.05$) compared with the empty liposome and control siRNA-DOPC groups (Fig. 5A). TUNEL staining showed that combination therapy resulted in a 72% increase in tumor cell apoptosis ($P < 0.001$) compared with empty liposome or control siRNA-DOPC groups and a 52% increase compared with ATP7B siRNA-DOPC alone (Fig. 5B). The RMG2 model had similar effects of therapy on proliferation and apoptosis (data not shown).

Because of growing evidence that copper plays an important role in angiogenesis (41), we examined MVD in ATP7B siRNA–treated tumors by CD31 staining. ATP7B siRNA-DOPC alone reduced MVD by 58% ($P < 0.05$), and combination therapy further reduced MVD by 81% ($P < 0.001$; Fig. 5C) compared with control groups. Based on the role of copper in regulating VEGF (42), we also examined tumor copper and VEGF content following ATP7B silencing. There was a 47% decrease ($P < 0.02$) in tumor copper content following ATP7B silencing (data not shown). ATP7B siRNA-DOPC alone reduced VEGF content by 75% ($P < 0.05$), and combination therapy further reduced it by 89% compared with the empty liposome–treated tumors ($P < 0.001$; Fig. 5D).

Discussion

We show here that *in vitro* ATP7B gene silencing leads to increased sensitivity to cisplatin in both parental and cisplatin-resistant cell lines. ATP7B gene silencing using a highly efficient method for systemic siRNA delivery resulted in antitumor efficacy in a platinum-resistant model of ovarian cancer in mice. Addition of cisplatin to ATP7B siRNA-DOPC, but not control siRNA-DOPC, further reduced the tumor burden in these mice, indicating that the effects were not due to nonspecific siRNA toxicity. These findings may be explained based on a benefit resulting from the coadministration of both drugs working independently of each other and not

necessarily *in vivo* sensitization. The antitumor activity was accomplished through decreased tumor cell proliferation and MVD and increased apoptosis. To the best of our knowledge, this study provides the first *in vivo* evidence about the therapeutic efficacy of targeting ATP7B in combination with cisplatin in platinum-resistant ovarian cancer.

Given the central role of platinum-based chemotherapy in the treatment of many cancers, including ovarian cancer, strategies to circumvent inherent or acquired resistance are highly desirable. Death of tumor cells in response to chemotherapy is dependent on several factors, including the amount of drug that enters the cell and the nucleus, amount of DNA adduct formation, cell tolerability to DNA adducts, and the ability to repair DNA damage (43,44). Previously, Nakayama and associates (21,45) observed that the levels of ATP7B inversely correlated with cisplatin sensitivity in nine gynecologic cancer cell lines and that ovarian cancer patients with ATP7B expression had significantly poorer response to cisplatin-based chemotherapy than patients lacking detectable ATP7B expression. The contribution of ATP7B to cisplatin resistance is evident from the results of ATP7B down-regulation. Reduced expression of ATP7B achieved by siRNA knockdown resulted in a 2.5-fold enhancement of sensitivity of these cells to cisplatin. Significantly, the down-regulation of another Cu-ATPase ATP7A had no effect, emphasizing the important and specific role of ATP7B in resistance of A2780-CP20 cells to cisplatin.

The different effects of ATP7A and ATP7B silencing on cisplatin resistance may be linked to their different levels of expression and/or their distinct trafficking properties. In A2780-CP20 cells, ATP7A traffics toward the plasma membrane in response to copper elevation (data not shown), presumably to export excess metal out of the cell. In contrast, ATP7B shows no relocalization in response to either copper or cisplatin and is likely to sequester metals in the intracellular compartments. If in A2780-CP20 cells the ATP7A-mediated export of cisplatin is much slower than cisplatin uptake, then ATP7A inactivation would not have a significant effect on cisplatin resistance. In contrast, the concept that ATP7B controls intracellular distribution of cisplatin is supported by our observation that down-regulation of ATP7B does not significantly alter the cellular content of cisplatin, and yet, a 30% increase in DNA adduct formation is observed. This result reflects the increased nuclear availability of cisplatin in response to ATP7B down-regulation. Therefore, the major mechanism through which overexpression of ATP7B increases resistance to cisplatin seems to involve blockade of drug access to the nucleus. This may be due either to ATP7B pumping cisplatin into the lumen of the TGN or to simple binding of the drug by multiple metal-binding sites in the NH_2-terminal domain (N-ATP7B) of the transporter or both. The latter possibility is supported by our finding that the recombinant N-ATP7B alone increased cell resistance to cisplatin. While this work was in preparation, new *in vitro* data (showing that cisplatin stimulates the catalytic activity of ATP7B and that this stimulation requires the NH_2-terminal region) by Leonhardt and colleagues (46) provided additional evidence for the role of the NH_2-terminal metal-binding domain in functional interactions between cisplatin and ATP7B.

Despite efficient down-regulation of ATP7B in A2780-CP20 cells, reversal of the resistant phenotype was not complete, indicating possible involvement of other components of cellular copper handling machinery (such as high-affinity copper transporter hCTR1, metallochaperones, and ATP7B regulator COMMD1; ref. 47). Furthermore, changes in expression of Cu-ATPases alter the intracellular copper balance (17) and this in turn induces changes in the cell transcriptome (48). However, these additional mechanisms do not diminish the major contribution of ATP7B. The *in vivo* therapy with combination of ATP7B siRNA-DOPC and cisplatin significantly reduced tumor burden, decreased cell proliferation and MVD, and increased apoptosis, suggesting that this approach might be useful in patients with platinum-resistant ovarian carcinoma. Copper plays an important role in angiogenesis and it might be a required cofactor of VEGF-mediated angiogenesis (42). Copper stimulates the

proliferation and migration of endothelial cells and is required for the secretion of several angiogenic factors by tumor cells. Copper may bind to angiogenic growth factors or regulate the production of angiogenic growth factors such as VEGF (42). Thus, therapy aimed at depleting copper levels through silencing the transporters may have an additional benefit by reducing angiogenesis. In summary, our data indicate that ATP7B-targeted therapy may represent a novel therapeutic approach for platinum-resistant human ovarian cancer.

Supplementary Material

Refer to Web version on PubMed Central for supplementary material.

Acknowledgments

We thank Robert R. Langley, Donna Reynolds, and Fang Wang for their technical expertise and helpful discussion.

Grant support: Program Project Development Grant from the Ovarian Cancer Research Fund, Inc., the Zarrow Foundation, the University of Texas M. D. Anderson Ovarian Cancer Specialized Program of Research Excellence grant P50 CA 083639, the Betty Ann Asche Murray Distinguished Professorship, and the Marcus Foundation (A.K. Sood); National Cancer Institute F31CA126474 Fellowship for Minority Students award (G.N. Armaiz-Pena); NIH-sponsored Women's Reproductive Health Research grant HD050128 through Baylor College of Medicine (M.M.K. Shahzad); National Cancer Institute-Department of Health and Human Services NIH 32 Training grant T32 CA101642 (Y.G. Lin and A.M. Nick); NIH grant DK071865 (S. Lutsenko, V. Zuzel, and E.S. Leshane); and NIH grant CA16672 (Z.H. Siddik).

References

1. Jemal A, Siegel R, Ward E, Murray T, Xu J, Thun MJ. Cancer statistics, 2007. CA Cancer J Clin 2007;57:43–66. [PubMed: 17237035]
2. McGuire WP, Hoskins WJ, Brady MF, et al. Cyclophosphamide and cisplatin compared with paclitaxel and cisplatin in patients with stage III and stage IV ovarian cancer. N Engl J Med 1996;334:1–6. [PubMed: 7494563]
3. Sood AK, Buller RE. Drug resistance in ovarian cancer: from the laboratory to the clinic. Obstet Gynecol 1998;92:312–9. [PubMed: 9699774]
4. Leyland-Jones B, Kelland LR, Harrap KR, Hiorns LR. Genomic imbalances associated with acquired resistance to platinum analogues. Am J Pathol 1999;155:77–84. [PubMed: 10393840]
5. Kelland LR. Preclinical perspectives on platinum resistance. Drugs 2000;59:1–8. [PubMed: 10864225] discussion 37–8
6. Perez RP. Cellular and molecular determinants of cisplatin resistance. Eur J Cancer 1998;34:1535–42. [PubMed: 9893624]
7. Kruh GD. Lustrous insights into cisplatin accumulation: copper transporters. Clin Cancer Res 2003;9:5807–9. [PubMed: 14676099]
8. Weinstein RS, Kuszak JR, Kluskens LF, Coon JS. P-glycoproteins in pathology: the multidrug resistance gene family in humans. Hum Pathol 1990;21:34–48. [PubMed: 1967244]
9. Douple EB. *cis*-Diamminedichloroplatinum(II): effects of a representative metal coordination complex on mammalian cells. Pharmacol Ther 1984;25:297–326. [PubMed: 6542679]
10. Lage H, Dietel M. Involvement of the DNA mismatch repair system in antineoplastic drug resistance. J Cancer Res Clin Oncol 1999;125:156–65. [PubMed: 10235469]
11. Samimi G, Fink D, Varki NM, et al. Analysis of MLH1 and MSH2 expression in ovarian cancer before and after platinum drug-based chemotherapy. Clin Cancer Res 2000;6:1415–21. [PubMed: 10778972]
12. Ooi CE, Rabinovich E, Dancis A, Bonifacino JS, Klausner RD. Copper-dependent degradation of the *Saccharomyces cerevisiae* plasma membrane copper transporter Ctr1p in the apparent absence of endocytosis. EMBO J 1996;15:3515–23. [PubMed: 8670854]

13. Katano K, Safaei R, Samimi G, Holzer A, Rochdi M, Howell SB. The copper export pump ATP7B modulates the cellular pharmacology of carboplatin in ovarian carcinoma cells. Mol Pharmacol 2003;64:466–73. [PubMed: 12869652]
14. Katano K, Kondo A, Safaei R, et al. Acquisition of resistance to cisplatin is accompanied by changes in the cellular pharmacology of copper. Cancer Res 2002;62:6559–65. [PubMed: 12438251]
15. Qian Y, Tiffany-Castiglioni E, Harris ED. Copper transport and kinetics in cultured C6 rat glioma cells. Am J Physiol 1995;269:C892–8. [PubMed: 7485458]
16. Katano K, Safaei R, Samimi G, et al. Confocal microscopic analysis of the interaction between cisplatin and the copper transporter ATP7B in human ovarian carcinoma cells. Clin Cancer Res 2004;10:4578–88. [PubMed: 15240550]
17. Samimi G, Safaei R, Katano K, et al. Increased expression of the copper efflux transporter ATP7A mediates resistance to cisplatin, carboplatin, and oxaliplatin in ovarian cancer cells. Clin Cancer Res 2004;10:4661–9. [PubMed: 15269138]
18. Ohbu M, Ogawa K, Konno S, et al. Copper-transporting P-type adenosine triphosphatase (ATP7B) is expressed in human gastric carcinoma. Cancer Lett 2003;189:33–8. [PubMed: 12445675]
19. Kanzaki A, Toi M, Neamati N, et al. Copper-transporting P-type adenosine triphosphatase (ATP7B) is expressed in human breast carcinoma. Jpn J Cancer Res 2002;93:70–7. [PubMed: 11802810]
20. Higashimoto M, Kanzaki A, Shimakawa T, et al. Expression of copper-transporting P-type adenosine triphosphatase in human esophageal carcinoma. Int J Mol Med 2003;11:337–41. [PubMed: 12579336]
21. Nakayama K, Kanzaki A, Terada K, et al. Prognostic value of the Cu-transporting ATPase in ovarian carcinoma patients receiving cisplatin-based chemotherapy. Clin Cancer Res 2004;10:2804–11. [PubMed: 15102688]
22. Sugeno H, Takebayashi Y, Higashimoto M, et al. Expression of copper-transporting P-type adenosine triphosphatase (ATP7B) in human hepatocellular carcinoma. Anticancer Res 2004;24:1045–8. [PubMed: 15154620]
23. Miyashita H, Uchida T, Mori S, Echigo S, Motegi K. Expression status of Pin1 and cyclins in oral squamous cell carcinoma: Pin1 correlates with cyclin D1 mRNA expression and clinical significance of cyclins. Oncol Rep 2003;10:1045–8. [PubMed: 12792768]
24. Aida T, Takebayashi Y, Shimizu T, et al. Expression of copper-transporting P-type adenosine triphosphatase (ATP7B) as a prognostic factor in human endometrial carcinoma. Gynecol Oncol 2005;97:41–5. [PubMed: 15790435]
25. Vulpe C, Levinson B, Whitney S, Packman S, Gitschier J. Isolation of a candidate gene for Menkes disease and evidence that it encodes a copper-transporting ATPase. Nat Genet 1993;3:7–13. [PubMed: 8490659]
26. Bull PC, Thomas GR, Rommens JM, Forbes JR, Cox DW. The Wilson disease gene is a putative copper transporting P-type ATPase similar to the Menkes gene. Nat Genet 1993;5:327–37. [PubMed: 8298639]
27. Lutsenko S, Barnes NL, Bartee MY, Dmitriev OY. Function and regulation of human copper-transporting ATPases. Physiol Rev 2007;87:1011–46. [PubMed: 17615395]
28. Landen CN, Chavez-Reyes A, Bucana C, et al. Therapeutic EphA2 gene targeting *in vivo* using neutral liposomal small interfering RNA delivery. Cancer Res 2005;65:6910–8. [PubMed: 16061675]
29. Halder J, Kamat AA, Landen CN, et al. Focal adhesion kinase targeting using *in vivo* short interfering RNA delivery in neutral liposomes for ovarian carcinoma therapy. Clin Cancer Res 2006;12:4916–24. [PubMed: 16914580]
30. Sood AK, Seftor EA, Fletcher MS, et al. Molecular determinants of ovarian cancer plasticity. Am J Pathol 2001;158:1279–88. [PubMed: 11290546]
31. Halder J, Landen CN, Lutgendorf SK. Focal adhesion kinase silencing augments docetaxel-mediated apoptosis in ovarian cancer cells. Clin Cancer Res 2005;11:8829–36. [PubMed: 16361572]
32. Lutsenko S, Petrukhin K, Cooper MJ, Gilliam CT, Kaplan JH. N-terminal domains of human copper-transporting adenosine triphosphatases (the Wilson's and Menkes disease proteins) bind copper selectively *in vivo* and *in vitro* with stoichiometry of one copper per metal-binding repeat. J Biol Chem 1997;272:18939–44. [PubMed: 9228074]

33. Killion JJ, Radinsky R, Fidler IJ. Orthotopic models are necessary to predict therapy of transplantable tumors in mice. Cancer Metastasis Rev 1998;17:279–84. [PubMed: 10352881]
34. Voskoglou-Nomikos T, Pater JL, Seymour L. Clinical predictive value of the *in vitro* cell line, human xenograft, and mouse allograft preclinical cancer models. Clin Cancer Res 2003;9:4227–39. [PubMed: 14519650]
35. Kim TJ, Ravoori M, Landen CN, et al. Antitumor and antivascular effects of AVE8062 in ovarian carcinoma. Cancer Res 2007;67:9337–45. [PubMed: 17909042]
36. Bartee MY, Lutsenko S. Hepatic copper-transporting ATPase ATP7B: function and inactivation at the molecular and cellular level. Biometals 2007;20:627–37. [PubMed: 17268820]
37. Lutsenko S, LeShane ES, Shinde U. Biochemical basis of regulation of human copper-transporting ATPases. Archiv Biochem Biophys 2007;463:134–48.
38. DiDonato M, Narindrasorasak S, Forbes JR, Cox DW, Sarkar B. Expression, purification, and metal binding properties of the N-terminal domain from the Wilson disease putative copper-transporting ATPase (ATP7B). J Biol Chem 1997;272:33279–82. [PubMed: 9407118]
39. Walker JM, Huster D, Ralle M, Morgan CT, Blackburn NJ, Lutsenko S. The N-terminal metal-binding site 2 of the Wilson's disease protein plays a key role in the transfer of copper from Atox1. J Biol Chem 2004;279:15376–84. [PubMed: 14754885]
40. Li SD, Chen YC, Hackett MJ, Huang L. Tumor-targeted delivery of siRNA by self-assembled nanoparticles. Mol Ther 2007;161:163–169. [PubMed: 17923843]
41. Lowndes SA, Harris AL. The role of copper in tumour angiogenesis. J Mamm Gland Biol Neoplasia 2005;10:299–310.
42. Goodman VL, Brewer GJ, Merajver SD. Control of copper status for cancer therapy. Curr Cancer Drug Targets 2005;5:543–9. [PubMed: 16305350]
43. Andrews PA, Howell SB. Cellular pharmacology of cisplatin: perspectives on mechanisms of acquired resistance. Cancer Cells 1990;2:35–43. [PubMed: 2204382]
44. Siddik ZH. Cisplatin: mode of cytotoxic action and molecular basis of resistance. Oncogene 2003;22:7265–79. [PubMed: 14576837]
45. Nakayama K, Kanzaki A, Ogawa K, Miyazaki K, Neamati N, Takebayashi Y. Copper-transporting P-type adenosine triphosphatase (ATP7B) as a cisplatin based chemoresistance marker in ovarian carcinoma: comparative analysis with expression of MDR1, MRP1, MRP2, LRP and BCRP. Int J Cancer 2002;101:488–95. [PubMed: 12216079]
46. Leonhardt K, Gebhardt R, Mossner J, Lutsenko S, Huster D. Functional interactions of CU-ATPase ATP7B with cisplatin and the role of ATP7B in cells resistance to the drug. J Biol Chem 2009;284:7793–802. [PubMed: 19141620]
47. Komatsu M, Sumizawa T, Mutoh M, et al. Copper-transporting P-type adenosine triphosphatase (ATP7B) is associated with cisplatin resistance. Cancer Res 2000;60:1312–6. [PubMed: 10728692]
48. Huster D, Purnat TD, Burkhead JL, et al. High copper selectively alters lipid metabolism and cell cycle machinery in the mouse model of Wilson disease. J Biol Chem 2007;282:8343–55. [PubMed: 17205981]

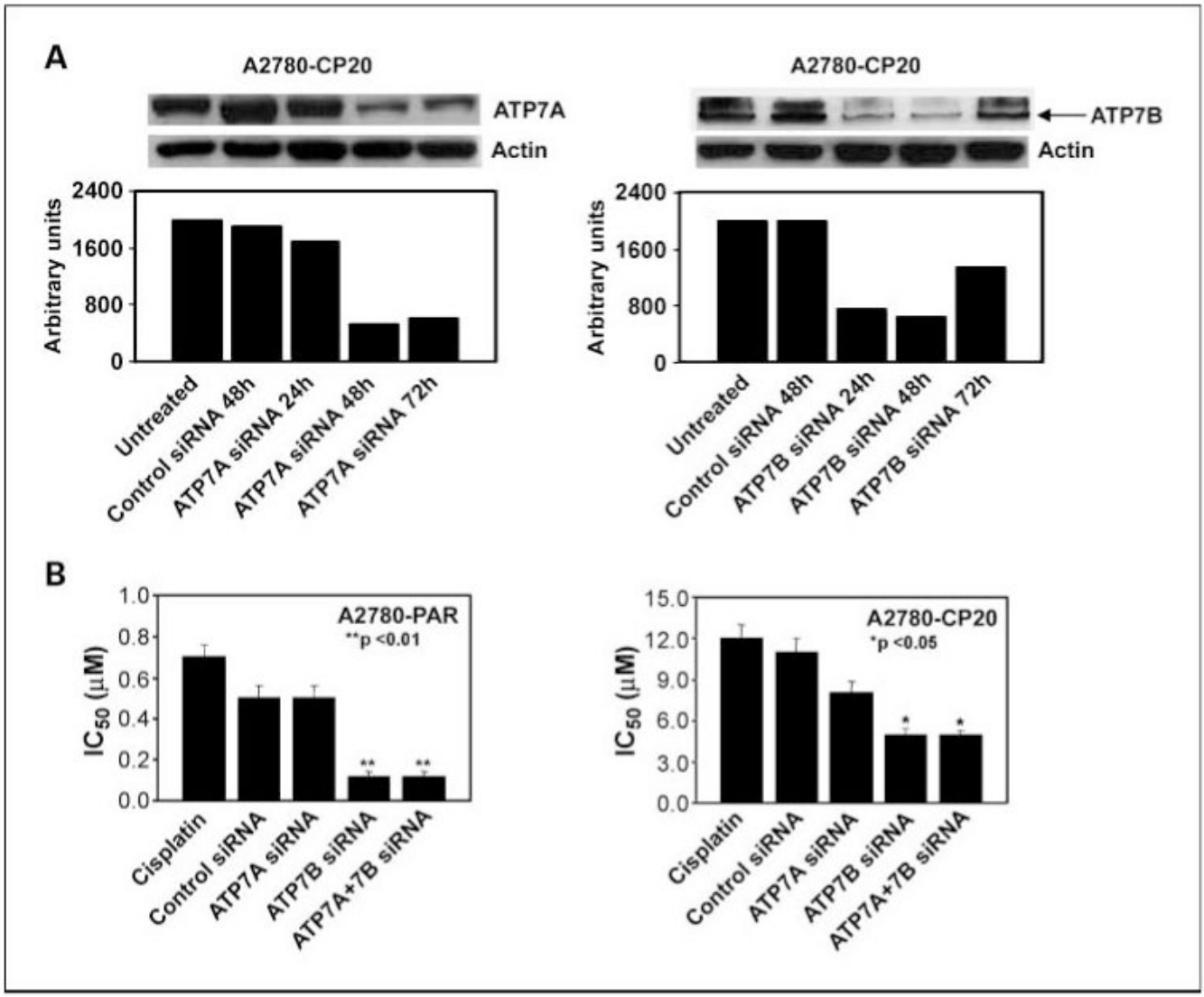

Fig. 1.

A, Western blot analysis of ATP7A and ATP7B in A2780-CP20 cells following treatment with targeted and control siRNA for 24, 48, and 72 h. β-Actin was used as loading control. Protein levels were quantified by densitometry and expression is shown as arbitrary units. *B*, effect of ATP7A and ATP7B silencing on cisplatin sensitivity in ovarian cancer cell lines. A2780-PAR and A2780-CP20 cells were transfected with ATP7A or ATP7B or control siRNA. After 24 h, cells were treated with cisplatin (0.01-32 μmol/L). Following 72 h of cisplatin exposure, MTT assay was done to determine the effects on cell viability. Columns, mean values for the IC_{50} of three independent experiments; bars, SE. *, $P < 0.05$; **, $P < 0.01$, compared with cisplatin alone.

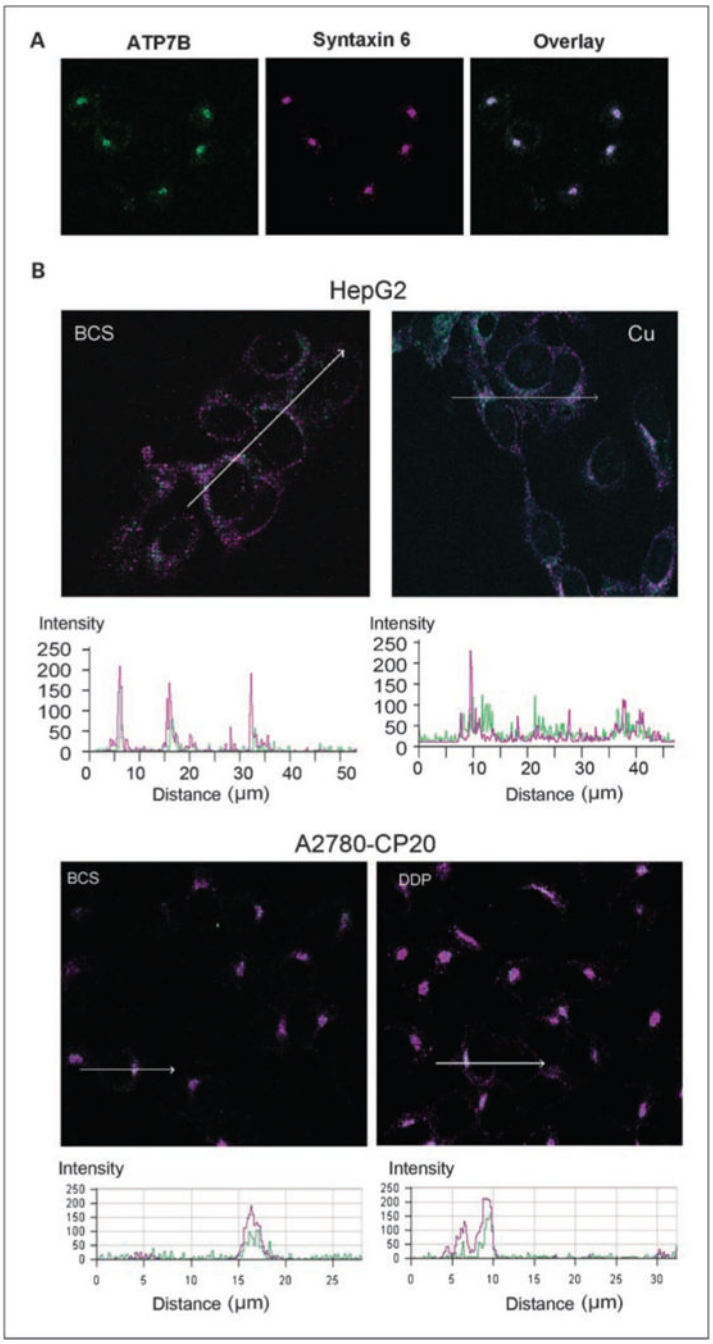

Fig. 2.

Effect of cisplatin on intracellular localization of ATP7B. *A,* A2780-CP20 cells were immunostained with the anti-ATP7B and anti–syntaxin-6 antibodies. Overlay images showing colocalization (*white*) of ATP7B (*green*) and syntaxin-6 (*pink*). *B,* HepG2 and A2780-CP20 cells were treated with copper chelator BCS (50 μmol/L) to deplete cells of copper and then either kept in BCS or treated with $CuCl_2$ or cisplatin. To verify the lack of ATP7B trafficking in response to cisplatin in A2780-CP20 cells, we evaluated colocalization between ATP7B and syntaxin using multiple images and Zeiss software package. Trafficking in response to copper in HepG2 was used as a positive control. Arrows indicate direction and length of the densitometry scan.

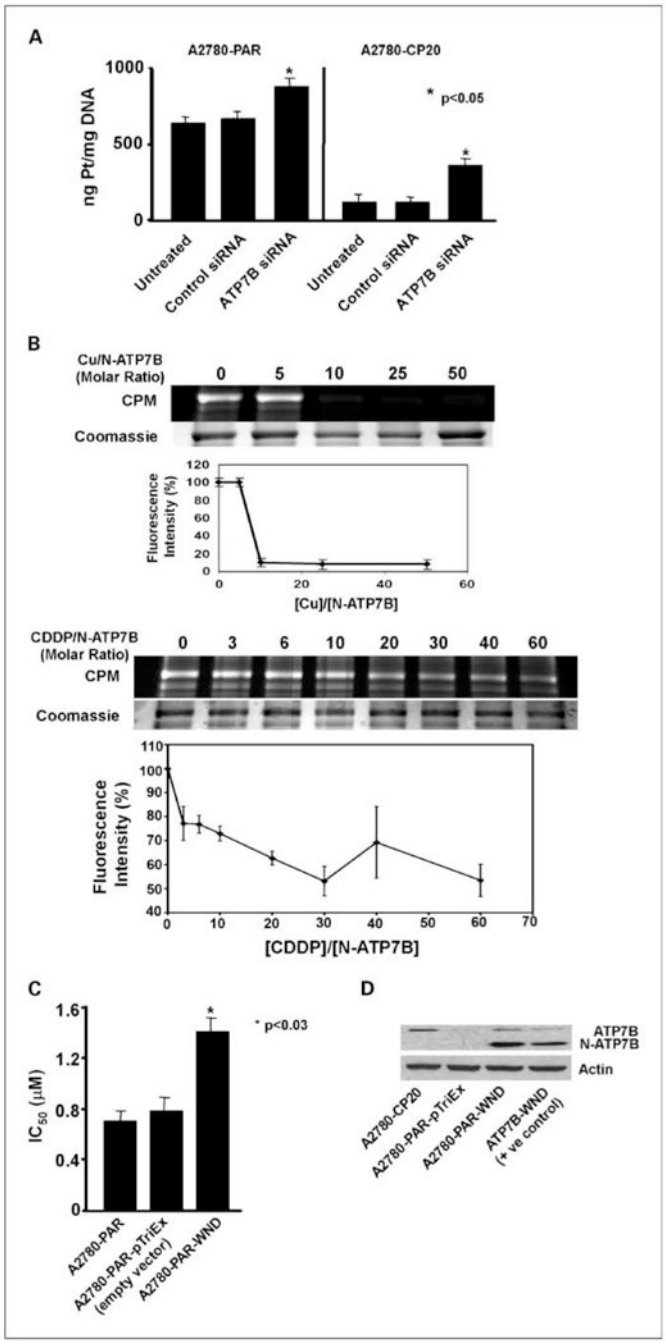

Fig. 3.

Effect of ATP7B gene silencing on DNA adduct formation in A2780-sensitive and A2780-resistant cells. *A*, the platinum content was determined using flame atomic absorption spectrometer after incubating A2780-PAR and A2780-CP20 cells with cisplatin for 4 h followed by digestion with 1 mol/L benzethonium hydroxide and acidification with 1 N HCl. Columns, mean values from three independent experiments; bars, SE. *, $P < 0.05$, compared with untreated or control siRNA–treated cells. *B*, cisplatin binds to the NH_2-terminal domain of ATP7B (N-ATP7B). The recombinant NH_2-terminal domain of ATP7B was incubated with increasing concentrations of copper or cisplatin (copper and cisplatin were added to the N-ATP7B in increasing molar ratios up to 60-fold excess over protein). Metal-coordinating

cysteines in N-ATP7B were labeled with cysteine-directed probe CPM. Top, copper/cisplatin protects against labeling with the CPM without affecting total amount of protein; bottom, fluorescence intensity for average of three replicates, defining 100% as the fluorescence/protein ratio where no ligand was used before labeling. The densitometry of fluorescent gels indicates that this protection is partial and hence not all metal-binding sites in the N-ATP7B bind cisplatin. *C*, overexpression of N-ATP7B increases cisplatin resistance in platinum-sensitive cells. A2780-PAR cells were transfected with empty vector pTriEx-cDNA or pTriEx-N-ATP7B cDNA (WND cDNA) using Lipofectamine 2000. After 48 h, cells were incubated with cisplatin (2 μmol/L) for 72 h at 37°C, and MTT assay was done to determine the difference in the IC_{50} levels. Columns, mean values for the IC_{50} of three independent experiments; bars, SE. *, $P < 0.03$, compared with A2780-PAR cells. *D*, Western blot analysis of overexpression of NH_2-terminal domain of ATP7B in A2780-PAR cells. Cells were transfected with pTriEx-cDNA or pTriEx-N-ATP7B cDNA as mentioned above and proteins were separated by SDS gel electrophoresis. β-Actin was used as loading control.

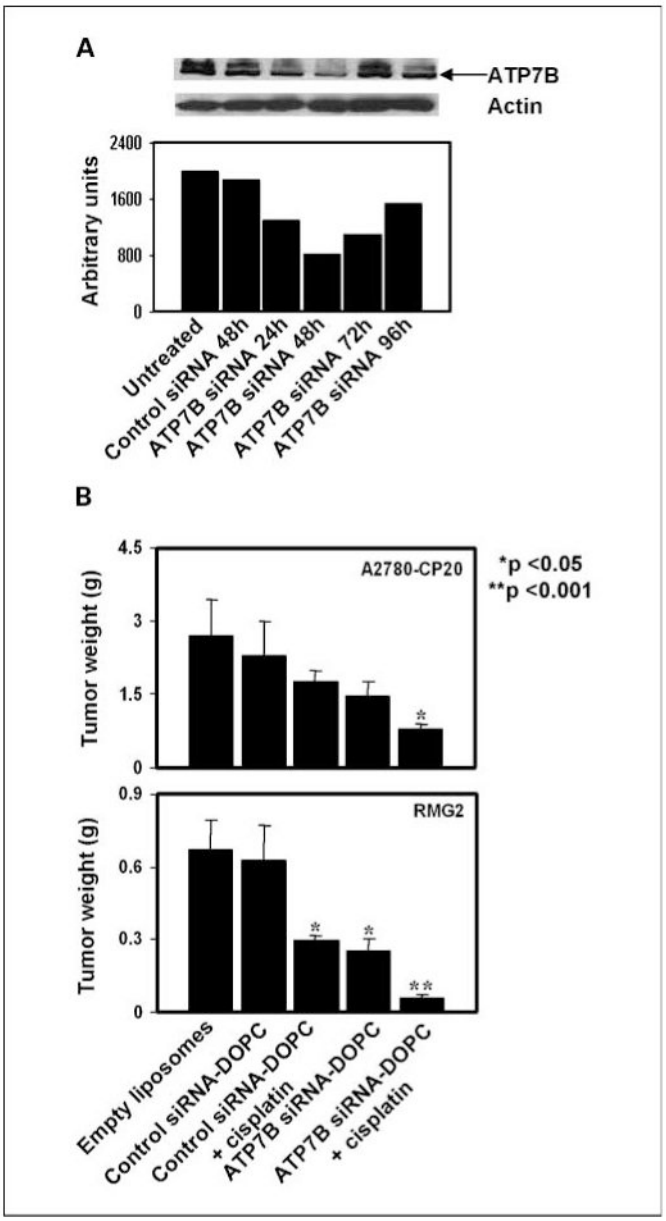

Fig. 4.

Effect of ATP7B gene silencing on ovarian carcinoma. *A*, Western blot of lysates from orthotopic tumor samples collected at 0, 1, 2, 3, and 4 d after a single administration of ATP7B siRNA or control siRNA incorporated in DOPC. Protein levels were quantified by densitometry and expression is shown as arbitrary units. *B*, therapeutic efficacy of siRNA-mediated ATP7B down-regulation. Nude mice were injected i.p. with 1.0×10^6 A2780-CP20 or 3.0×10^6 RMG2 cells and randomly allocated to one of the following groups: empty liposome, control siRNA-DOPC, control siRNA-DOPC + cisplatin, ATP7B siRNA-DOPC, and ATP7B siRNA-DOPC + cisplatin. Treatments were started 1 wk after tumor cell injection and siRNA/liposomes were administered twice weekly at a dose of 150 μg/kg body weight. All of the animals were sacrificed when animals in any group appeared moribund (A2780-CP20, after 3 wk; RMG2, 5 wk starting therapy) and necropsy was done and mouse weight, tumor weight, and location were recorded. Statistical analysis for tumor weights was done by

Student's *t* test. *, $P < 0.05$, compared with empty liposome or control siRNA-DOPC; **, $P < 0.001$, compared with control siRNA-DOPC + cisplatin or ATP7B siRNA-DOPC.

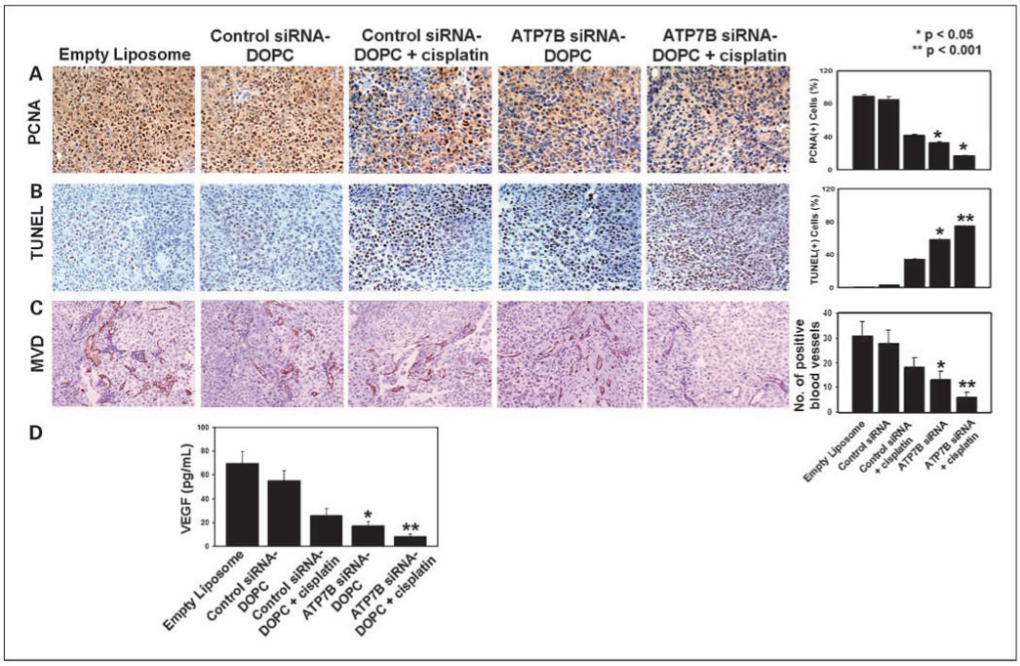

Fig. 5.

ATP7B gene silencing leads to reduced proliferation, increased apoptosis, and reduced MVD of A2780-CP20 tumors. Immunohistochemical staining for PCNA (*A*), TUNEL assay (*B*), and MVD (*C*) was conducted to assess cell proliferation, apoptosis, and MVD in A2780-CP20 tumors collected at completion of ATP7B siRNA-DOPC therapy. Original magnification, ×100. Quantification of effects is shown graphically on the right. Bars, 95% confidence intervals. Treatment arms were compared by Student's *t* test. *, $P < 0.05$; **, $P < 0.001$, compared with the empty liposome or control siRNA-DOPC groups. *D*, ATP7B silencing decreased VEGF levels in tumors. ELISA of A2780-CP20 tumors harvested at the completion of ATP7B therapy with or without cisplatin. Experiment was done twice. *, $P < 0.05$; **, $P < 0.001$, compared with empty liposome group.

Table 1

Characteristics of tumors after ATP7B siRNA-DOPC treatment with or without chemotherapy

Cell line	Treatment	Median no. nodules (range)	*P* (vs control)
A2780-CP20	Empty liposome	22 (4-63)	
	Control siRNA	24 (15-56)	ns
	Control siRNA + cisplatin	19 (6-39)	ns
	ATP7B siRNA	13 (1-37)	0.02
	ATP7B siRNA + cisplatin	8 (3-33)	0.05
RMG2	Empty liposome	12 (4-25)	
	Control siRNA	12 (4-21)	ns
	Control siRNA + cisplatin	8.5 (2-18)	ns
	ATP7B siRNA	7 (5-10)	0.02
	ATP7B siRNA + cisplatin	2.5 (1-6)	0.05

Abbreviation: ns, not significant.